JOURNAL OF FORENSIC SCIENCES

J Forensic Sci, May 2012, Vol. 57, No. 3
doi: 10.1111/j.1556-4029.2011.01988.x
Available online at: onlinelibrary.wiley.com

TECHNICAL NOTE

ENGINEERING SCIENCES

Daiqin Tao,[1] *Ph.D.; Zhiyong Yin,*[1] *Ph.D.; Hui Zhao,*[1] *Ph.D.; and Shengxiong Liu,*[1] *Ph.D.*

The Experimental and Case Study of Needle Marks on the Speedometer as the Physical Evidence for the Collision Speed Analysis*

ABSTRACT: The collision speed is important in accident analysis, and needle marks can be helpful as the physical evidence. The deceleration impact system has been built to analyze the mechanics of the needle and the gauge plate. Two isolated groups were designed to record the speed values under the same sample labels from real crashes. The visualization platform was built for the first group to collect needle marks. The second group recorded the speed values by other methods. The collision deceleration, the gauge plate materials, and the collision directions determine the forming of the needle marks. There were eight positive results from the 23 effective samples (12 frontal, four side, and seven rear), with discernible tip and/or middle marks on gauge plates. Multiple marks have been distinguished effectively. The low- and high-speed impacts have no obvious differences for real needle marks. It is more accurate for frontal impacts.

KEYWORDS: forensic science, traffic accident analysis, physical evidence, collision speed, speedometer, needle marks

As a major cause of death and disability (1), traffic accidents have become the world's largest public nuisance. As the speed is an important determinant of injury (2), the collision speed determination can be of considerable importance in traffic accidents analysis (3).

Although there are a number of techniques proposed to carry out such investigations, such as skid-mark analysis (4), deflection analysis (5), and pedestrian-thrown estimation (6) or objects calculation (7), the practical conditions are more or less limited (8) to interfere these traditional methods to be the optimal approaches. Therefore, new experimental methods (9), as well as image analysis (10–12), video analysis (13,14), and computer simulations (15–18), have been suggested. These new approaches have improved the accurateness of speed determination (19), but their uncertainties have been criticized (19,20). Moreover, some experts (21,22) have utilized the score marks or scratches on the tires or bodies of the vehicles to estimate the speed. Although these calculations have solved parts of the problem, they are rather complicated in the real work.

Theories of the physical evidence enlighten a new direction based on needle marks on the speedometer. Based on the Locard's exchange principle (23), these marks have been found to be a kind of physical evidence (24) but of little attention for them.

It may be considered that the technological innovation has washed out the research need for the needle marks. For the concept of event data recorders (EDRs) (25), which are now installed in many vehicles and will shortly be mandated in all new vehicles sold in the U.S.A., they can take records of accidents or events. Therefore, they could eliminate the need for reliance on other reconstruction analyses. What is more, the electronic speedometers cannot be analyzed for needle slap. And such speedometers have been commonly installed in many vehicle models worldwide. But the reality is that these are only for the developed and some for the developing areas. And sometimes the analyzers could not take the EDRs away without permission. While for more of the developing and most of the undeveloped regions, the traditional mechanical speedometers are the broad reality for them. The modern researchers have abandoned this speedometer type, but they are suffering the same rate of accidents or more.

Therefore, these lead to the situation of the absence and necessity of experimental and case studies on the needle marks as a simple and accurate way for collision speed determination.

The basic function of the speedometer is to indicate the driving speed. There are two kinds of speedometers. One is the mechanical, and the other is the electronic. In this research, only the former one has been studied. During the collision, the needle hanging over the gauge plate may leave marks like fingerprint and show the impacting speed exactly. For many decades, automotive, aircraft, and industrial engineers and accident reconstructionists have often looked for this type of evidence in a variety of accident situations involving mechanical gauges.

In this research, based on the laboratory impact system and mechanical analysis, two potential locations of the needle marks, the tip and the middle, have been revealed. The morphological characteristics have been collected under multiband light waves on real crashes marks. The precision and limitations have also been discussed by the real crashes data.

Materials and Methods

Impact System

A mechanical speedometer (5C 83010-3A320 157320-7420 956) was randomly obtained from a real car (Santana 2000; Volkswagen Aktiengesellschaft, Wolfsburg, Germany) as a laboratory sample.

[1]Research Institute for Traffic Medicine, Daping Hospital, Third Military Medical University, Chongqing 400042, China.

*Supported by the National Natural Science Foundation of China (30800243, 31170908, and 81072504), and the Natural Science Foundation of Chongqing of China (CSTC.2005BA6020, CSTC.2005AB6022, and CSTC.2009AB208).

Received 17 Aug. 2010; and in revised form 16 Jan. 2011; accepted 22 Jan. 2011.

The impact system was designed to simulate the needle movement during collision, to make clear the details of the forming of the marks.

The impacting system mainly included the components as shown in Fig. 1. The movable plate could slide through the guide rails and then impacted on the fixed lower bracket. The speedometer was clamped on the movable plate with ropes that were fixed on the base of the movable plate. Besides, the speedometer contacted the ropes slightly so as to maximally eliminate the disturbing force coming from the movable plate, thus making the speedometer relatively free to move along the movable plate and hit vertically to the lower bracket. Under the bottom of the speedometer, there was a cushion (5.0 ± 0.1 mm) on the base of the movable platform which to some extent was used to protect the speedometer but of little influence (26) to the inner mechanical structure.

Preparation

First, with the poles and the cover, the speedometer was clamped on the movable plate with its bottom side parallel to the movable plate.

Then, the accelerometer (model: 52M31-2000-10-240; dimension: 9.0 mm × 4.5 mm × 2.5 mm; weight: 0.5 g; sensitivity: 0.1512 mV/g; Measurement Specialties., Inc., Jiangsu, China) was attached horizontally and firmly with strong agglutinant (Modified Acrylate Adhesive; Geliahao Group, Fushun, China) to the fixed edge of the speedometer model just oppositely to the impacting point to minimize the error.

Finally, the Synergy P Portable Data Acquisition System (sample rate: 10 kHz; Hi-Techniques, Inc., Madison, WI) was configured to ready to obtain the g-data.

Test Procedure

At the beginning, the movable plate was lifted to a position of 0.50 ± 0.01 m height away from the fixed lower bracket. Then, the intensity and direction of the lamplight were adjusted until the pictures could be seen clearly on the high-speed video camera (Phantom v4.3, 5000 fps; Vision Research, Inc., Wayne, NJ). After this, the movable plate was made to fall free along the guide rails. The trigger of the high-speed video camera and the trigger of the data acquisition system were switched on through two shunt-wound triggering signal wires to record the impacting process synchronously.

Then, the height of the initial position of the movable plate was lifted at 2.90 ± 0.01 m (the maximal height of the impact system). Data were obtained in the same way.

In the experiments, the g-history and the impact video were obtained using the set up and method described earlier. The serial frames could be extracted from the video. Image processing was taken by the image software (Adobe Photoshop CS4; Adobe Systems, Inc., San Jose, CA) to observe the details.

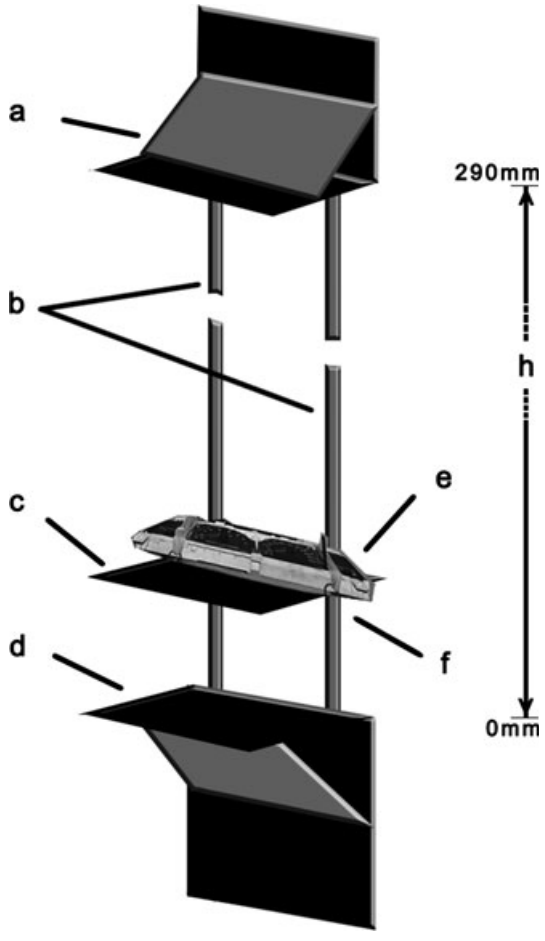

FIG. 1—*Impact system: (a) the fixed upper bracket, (b) the fixed guide rails, (c) the movable plate, (d) the fixed lower bracket, (e) the speedometer, and (f) the cushion.*

Real Marks Detection

There were two groups. The first group was responsible for image collection and speed reading from the gauge plate, while the second group obtained the speed values by other lawful methods to the national standard (GA/T643-2006; The Speed Technical Evaluation for Vehicles Involved in Representative Road Accidents, Beijing, China) including skid-mark analysis, deflection analysis, and pedestrian-thrown estimation or objects calculation based on the conditions of the cases. The two groups were all required to provide the upper and the lower limits of the results rigorously as far as possible.

For the needle marks method as the first group, at first, speedometer samples (from March to October, 2010) of real cases were collected validly without contamination or preexisted accidents by checking the survey reports of the vehicles. Only label numbers of these samples were shared between the two groups. Each group recorded the speed values under the same labels without information exchange. Samples with effective results have been extracted to do further comparing tests.

Then, the image station was built in the standard black room. A photograph platform was set up to collect images. The images were taken by a digital camera (Canon G11; Canon, Inc., Tokyo, Japan) fixed on the shelf. The shelf could move up and down through the guide rail to adjust the height of the camera. The xenon lamp (PoliEye® Hand-Held Xenon Forensic Light Sources, ST55-13F; LongHope Police Equipment Co., Ltd., Beijing, China) was put outside the platform as a flexible light source. During the photographing, all bands were taken for observing the visualization effects under each band. The incident angels of the light source were adjusted. All bands were tested for the selection of the optimal combination. After that, all images were imported into the computer to observe their morphological details and to read the speed values. At last, comparing tests and statistics were taken under the effective labels.

Results and Discussion

The Impact Experimental Results

At the height of 0.50 m, the needle did not touch the surface of the gauge plate, while at the height of 2.90 m, the tip of the needle heavily hit the gauge plate and deformed obviously and elastically as shown in Fig. 2.

By the Newton's Laws of Motion, the impact speed from 0.50 m height was 3.13 m/s (≈11.27 km/h), while the impact speed from 2.90 m height was 7.54 m/s (≈27.14 km/h).

The total length of the needle was 0.525 ± 0.001 m. And the contact part of the needle was 0.010 ± 0.001 m. It was the tip part away from the fixed axis of the needle.

Falling free from the height of 2.90 ± 0.01 m as a positive result, there were two courses of collision during the process. One was the speedometer collision as the impact I, while the other was the needle-faceplate collision inside the speedometer as the impact II. The impact II determined the forming of needle marks. The gauge plate surface was deformed during the impact II.

There was a time lag between the two impacts as 0.0024 s counted by frame to frame from the high-speed video. There was only one touch between the needle and the gauge plate.

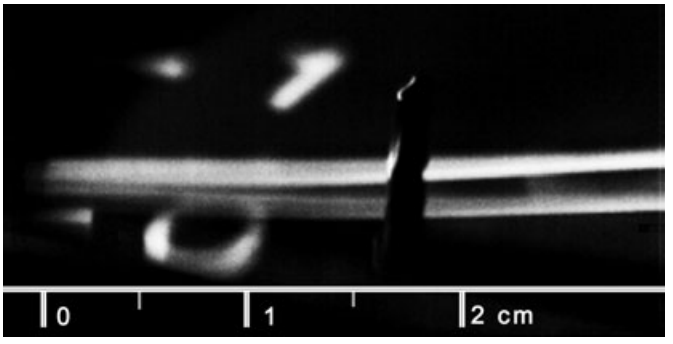

FIG. 2—*Collision moment: The needle tip is hitting the gauge plate and being deformed as free fall from the height of 2.90 m. It is a frame from the high-speed video.*

As shown in Fig. 3, as the needle-gauge plate collision happened at the point of B (0.0034 s, 250 g), with the time lag as 0.0024 s between these two impacts, the initial time of the impact I (the speedometer collision) should be at the point of A (0.001 s, 0 g).

The impulse (I) and the average reaction force (F) could be calculated as follows:

$$I = mv = m\sqrt{2gh} = \overline{F}t$$

Here, m was 0.860 ± 0.002 kg, h was 2.90 ± 0.01 m, and t was $(7 \pm 0.01) \times 10^{-3}$ s.

Therefore, the impulse of the impact was

$$I = 6.48 \pm 0.13\, N \cdot s$$

The average and peak reaction force in the experiments was

$$\overline{F} = 642.22 \pm 16\, N \text{ and } F_{\text{peak}} = |ma_{\text{peak}}| = 6152.44 \pm 1.46\, N$$

As the needle hitting the gauge plate at the point of B in Fig. 3, the force was 2700 ± 54 N. This force caused the impact II (the needle-faceplate impact).

Simply from the conservation law, the torque of the needle must resist to the torque of the axis from the gauge plate for equilibrium. So the needle vibrated up and down to find the chance to touch the gauge plate at the time point of B. It caused the impression shape by the heavy hitting of the needle tip to the gauge plate at the time point of B in Fig. 3 like a fingerprint.

The Morphological and Mechanical Analysis

As the tip marks have been obtained from the experiments, the mechanical structures between the needle and the gauge plate have been simply illustrated in Fig. 4 based on the high-speed video.

The experimental tip marks suggested the mechanical relationship as illustrated in Fig. 4*b*, and it has been verified by the real tip marks in Figs 5*a* and 6*c*.

Theoretically, there should be moving waves on the gauge plate surface as a curved plane. Therefore, any part on the curved plane

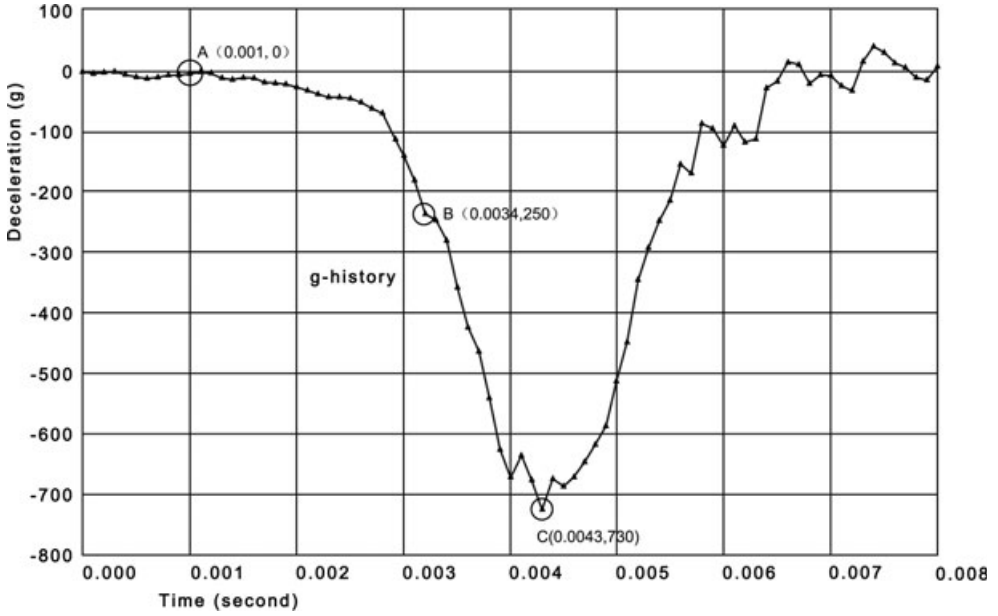

FIG. 3—*Deceleration waveform: free fall from 2.90 m with the peak value of the deceleration of 730 g. A: 0.001 s of time, 0 g of deceleration; B: 0.0034 s of time, −250 g of deceleration; and C: 0.0043 s of time, −730 g of deceleration.*

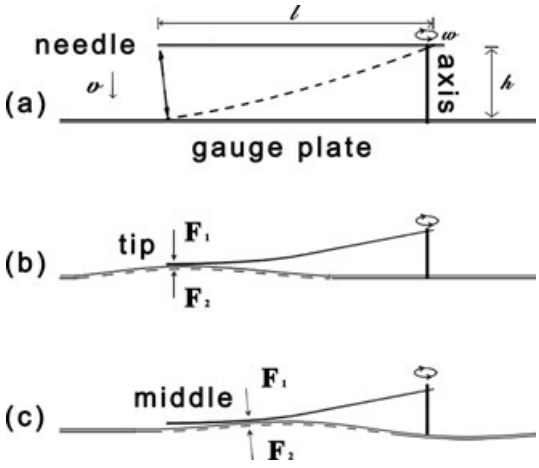

FIG. 4—*Mechanical diagram: (a) the mechanical relation among the needle, the axis, and the gauge plate; (b) the forming of the tip marks; and (c) the forming of the middle marks. Other situations could be deduced from (b) and (c).*

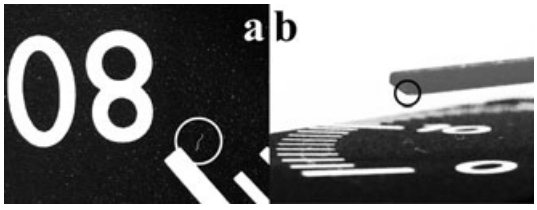

FIG. 5—*Label 100804-2: (a) the tip mark on the gauge plate (visualized under the normal white light); and (b) the tip of the needle. It is the number 5 (Label 100804-2) in Fig. 8.*

may come into being the ridge (/ridges) of vibration waves. So the needle may contact with the ridge (/ridges) and leave marks.

For the middle marks situations, the conjecture was that it might be the vibration from the needle like a beam with an overhanging end. But the needles were not long enough to generate such heavy deformation in the middle segments. So the middle marks could only be more caused by the deformation of the gauge plate material.

There were two cases (positive sample number 2 and 4 in Fig. 8) simultaneously left the tip and the middle marks in a separated form as one of them shown in Fig. 6. It has suggested the complicated higher-order vibrations of the gauge plate during the collision. The deformation could generate more complicated results that had not been obtained from the experiments, such as the simple middle type in Fig. 4*c*, which has been verified by real middle marks in Fig. 6*a*, or the multiple collision with multiple marks as shown in Fig. 7*b*. These middle marks were so typical that the morphological identification between the needles and the marks could be done accurately as shown in Fig. 6*b*.

For the multiple situations, the intensity of the impact energy could help to distinguish the sequence of the marks. As shown in Fig. 7*b*, the left marks were impressed prior to the right mark, because the left marks were more complete and deep than the right one, which indicated that it must be caused by the stronger impact that is the first and exact impact.

The Real Accidents Discussion

Although the data from the experiments and the real cases have eliminated the suspicion of the existence for the needle marks and have illustrated the mechanical functions and structures, the practical limitations should be discussed.

There were 23 effective labels (extracted from all the 57 random samples) with 12 frontal impacts, four side impacts (with two head-side impacts), and seven rear impacts. Among them, there were eight positive results (with discernible needle marks on gauge plates) which provided more unforeseen information that could not be easily obtained in the laboratory as shown in Fig. 8. To simplify the discussion, there were only two types of vehicle either in car or in motorcycle, for the geometrical model of their mechanics on the head. The vehicle type of car included the normal car, the van (Label 100804-2, 100908), the bus (Label 100625), and so on.

The maximum and minimum values in Fig. 8 are more or less influenced by χ (the deflection volume estimated from the deflection depth and width of the vehicle, GA/T643-2006) in the conventional and lawful standard practice. For each case, the deflection with the width and the depth had the maximum and the minimum values; thus, the speed values were various.

In the 34 ineffective cases, two of them lacked permission to take the speedometer away from the scene; 13 of them were

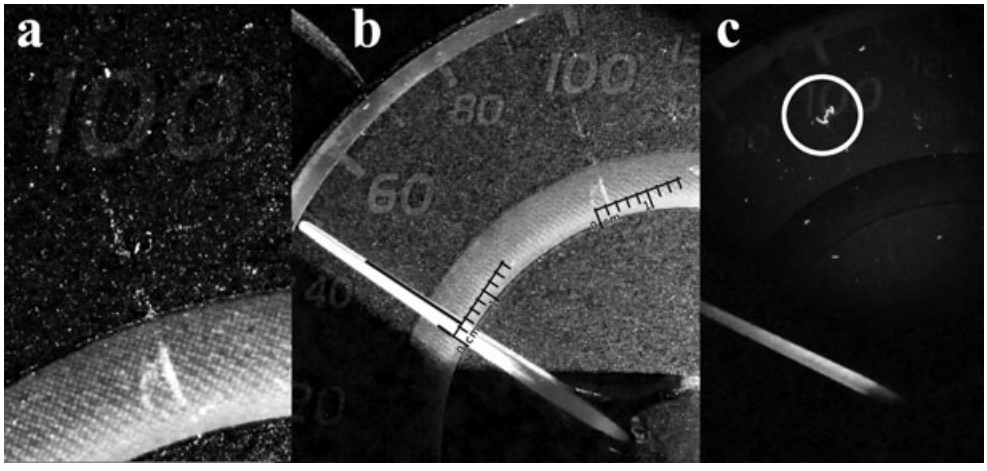

FIG. 6—*Label 100726: (a) the middle marks on the gauge plate (visualized under the blue light as 415-nm wave band); (b) the identification between the needle and the middle marks; and (c) the fluorescent tip marks (visualized under the ultraviolet as 365-nm wave band). It is the number 4 (Label 100726) in Fig. 8.*

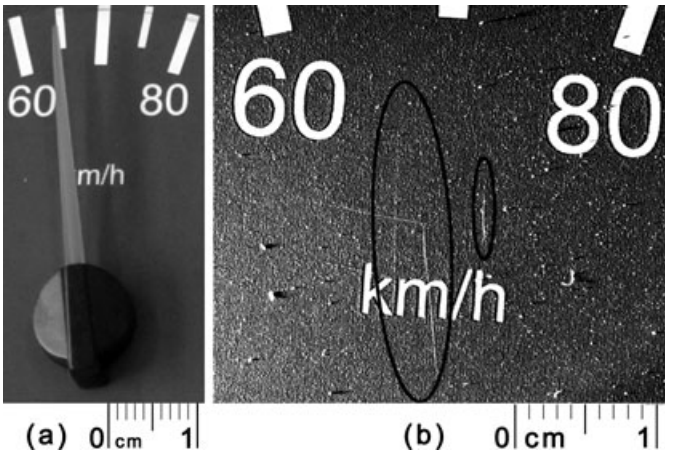

FIG. 7—*Label 100625: (a) the speedometer from the accident scene; (b) marks on the gauge plate (visualized under the normal torch light) that the left marks are positive while the right mark is negative; and (c) the middle marks of the needle on the gauge plate. It is the number 3 (Label 100625) in Fig. 8.*

contaminated by rain, blood, etc.; four of them had preaccidents; and nine of them were short of data for the estimation by the second group. While the needles of the other six samples were found blocked hanging over a certain scale on the gauge plate (like the situation in Fig. 7*a*) without impacting impressions detected, which could not be contained in the needle marks concept in this research. Therefore, all the 34 samples have been treated as ineffective.

Considering the 15 negative results under the 23 effective labels, detecting conditions have been back-checked. For the forming of the needle marks, the materials of the gauge plate influenced the forming of the needle marks more than the materials of the needle. The pretests on the odometers besides the speedometers obtained the bijection results that if there were the needle marks left on the odometers by the gently finger pressure, there were the needle marks on the speedometer and vice versa. Therefore, the back-checking for all the 15 negative samples showed that their needles could not leave any mark on the gauge plates or could not be detected under the current visualization condition.

For the eight positive samples under the frontal impact situations, the speed values read from the needle marks are valid and more precise than from the traditional methods as shown in Fig. 8. For needle marks, it needs to discuss their lower limits. For the lowest speed value as 42 km/h from the real sample 6, as well as the former experimental speed as about 27 km/h, the normal low-speed collision could also leave marks on the gauge plate. So the low-speed collisions should not be excluded when detecting for the needle marks. It does not mean that the traditional methods are of no use in practice, but means that the needle marks have been demonstrated as authentic and closer to the real collision speed, especially in the frontal impact situation.

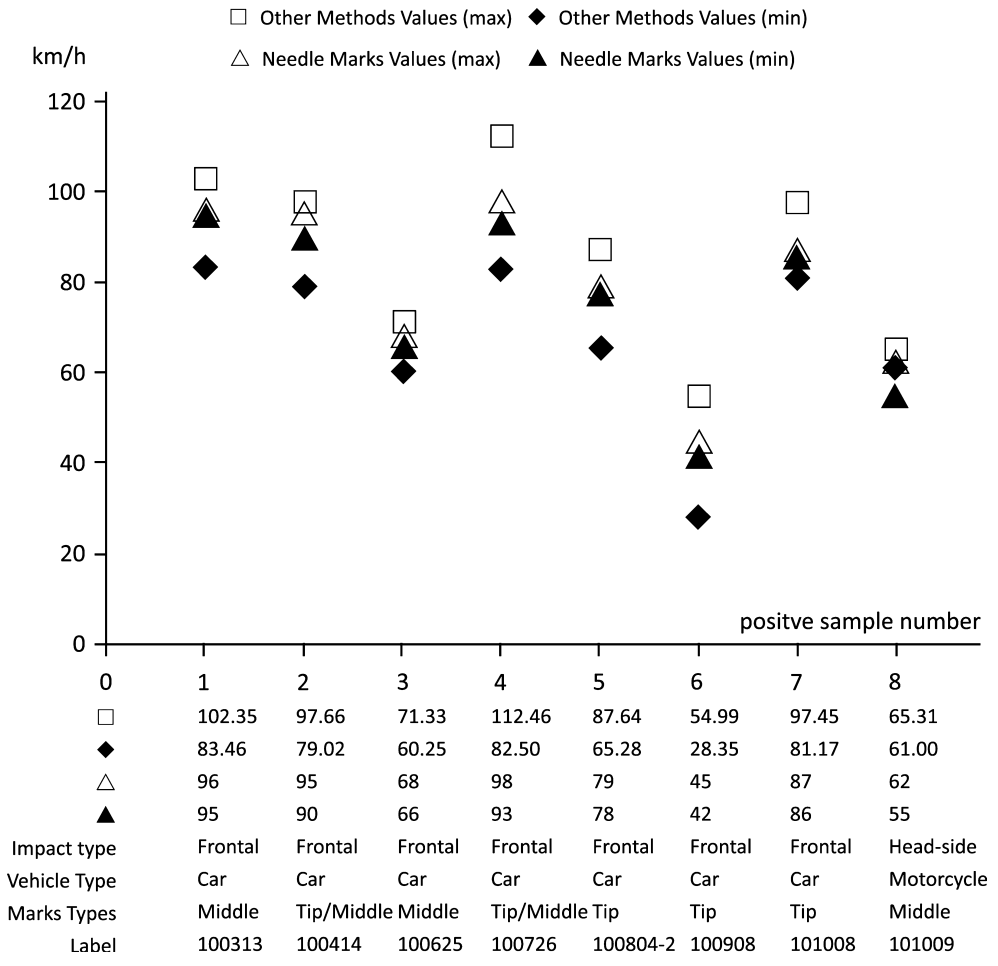

	0	1	2	3	4	5	6	7	8
□		102.35	97.66	71.33	112.46	87.64	54.99	97.45	65.31
◆		83.46	79.02	60.25	82.50	65.28	28.35	81.17	61.00
△		96	95	68	98	79	45	87	62
▲		95	90	66	93	78	42	86	55
Impact type		Frontal	Frontal	Frontal	Frontal	Frontal	Frontal	Frontal	Head-side
Vehicle Type		Car	Car	Car	Car	Car	Car	Car	Motorcycle
Marks Types		Middle	Tip/Middle	Middle	Tip/Middle	Tip	Tip	Tip	Middle
Label		100313	100414	100625	100726	100804-2	100908	101008	101009

FIG. 8—*Positive statistics: the eight positive results from the 23 effective real samples.*

Conclusions

From this research, it could conclude that:

• There are two potential locations for needle marks: one is the tip, and the other is the middle. They can appear either in a single form or in a together form. It depends on the collision situations.

• The needle marks are more likely to appear in the frontal impact situations than the others. And the deceleration and the gauge plate materials mainly influence the forming of the needle marks.

• There are no obvious differences between the low-speed and the high-speed impacts. But it is prominent that the needle marks from the frontal impacts are more precisely than from the traditional methods. The proposed method supports in roughly half of the frontal impacts and a few of the motorcycle impacts. While more details should be studied on rear and side impacts for further conclusions.

Acknowledgments

The authors wish to acknowledge the data supporting from the Chongqing Bayi Traffic Accident Appraisal Center of Judicature. The authors would also like to acknowledge the constructive comments given by the anonymous reviewers.

References

1. World Health Organization. Global status report on road safety: time for action. Geneva, Switzerland: World Health Organization, 2009.
2. Aarts L, Schagen I. Driving speed and the risk of road crashes: a review. Accid Anal Prev 2006;38:215–24.
3. Svenson O, Salo I. Effects of speed limit variation on judged mean speed of a trip. Accid Anal Prev 2010;42:704–8.
4. Lambourn RF. When vehicle speeds can be computed from skidmarks, and why. Int Crim Pol Rev 1979;325:48–53.
5. Tiwari V, Sutton M, McNeill SR. Assessment of high-speed imaging systems for 2D and 3D deformation measurements: methodology development and validation. Exp Mech 2007;47:561–79.
6. Evans AK, Smith R. Vehicle speed calculation from pedestrian throw distance. Proc Inst Mech Eng D J Auto Eng 1999;213:441–7.
7. Otte D. Use of throw distances of pedestrians and bicyclists as part of a scientific accident reconstruction method. SAE 2004 World Congress Exhibition; 2004 June 30. Detroit, MI: SAE International, 2004.
8. Simms CK, Wood DP, Walsh DG. Confidence limits for impact speed estimation from pedestrian projection distance. Int J Crashworthiness 2004;9:219–28.
9. Yin Z, Wang Z. Summary of basic research for traffic injury and judicial identification. International Congress Traffic Accident Investigation; 2009 Nov 5–6. Shanghai, China: Institution of Forensic Science of Ministry of Justice of China, 2009.
10. Lin HY, Lia KJ, Changa CH. Vehicle speed detection from a single motion blurred image. Image Vis Comput 2008;26:1327–37.
11. Buck U, Naether S, Braun M, Bolliger S, Friederich H, Jackowski C, et al. Application of 3D documentation and geometric reconstruction methods in traffic accident analysis: with high resolution surface scanning, radiological MSCT/MRI scanning and real data based animation. Forensic Sci Int 2007;170:20–8.
12. Zou Y, Shi G, Shi H, Wang Y. Image sequences based traffic incident detection for signaled intersections using hmm. Proceedings of the 2009 9th International Conference on Hybrid Intelligent Systems; 2009 Aug 12–14. Washington, DC: IEEE Computer Society, 2009.
13. Morris B, Trivedi M. Learning and classification of trajectories in dynamic scenes: a general framework for live video analysis. IEEE 5th International Conference—Advanced Video Signal Based Surveillance, 2008 Sept 1–3. Santa Fe, NM: AVSS, 2008.
14. Avinash N, Yadav DD, Murali S. Vision based relative speed detection of moving objects in a traffic environment. International Conference on Information and Multimedia Technololy; 2009 Dec 16–18. Jeju Island, South Korea: ICIMT, 2009.
15. Balazic J, Prebil I, Certanc N. Computer simulation of the accident with nine victims. Forensic Sci Int 2006;156:161–5.
16. Mei TX, Li H. Measurement of absolute vehicle speed with a simplified inverse model. IEEE T Veh Technol 2010;59:1164–71.
17. El-Murr G, Giaouris D, Finch JW. Totally parameter independent speed estimation of synchronous machines based on online short time fourier transform ridges. Eng Lett 2008;16:14.
18. Consoli A, Scarcella G, Testa A. Industry application of zero-speed sensorless control techniques for PM synchronous motors. IEEE T Ind Appl 2001;37:513–21.
19. Randles B, Jones B, Welcher J, Szabo T, Elliott D, MacAdams C. The accuracy of photogrammetry vs. hands-on measurement techniques used in accident reconstruction. SAE 2010 World Congress and Exhibition; 2010 April 13–15. Detroit, MI: SAE International, 2010.
20. Wach W, Unarski J. Uncertainty of calculation results in vehicle collision analysis. Forensic Sci Int 2007;167:181–8.
21. Levy RA. Speed determination in car-truck sideswipe collisions. SAE 2000 World Congress; 2000 March 6–9. Detroit, MI: SAE International, 2000.
22. Liu C, Li Y, Li B, Ma J. Velocity estimation fully depend on the scraped marks of tire. Auto Eng 2006;28:68–73.
23. Richard S. Criminalistics: an introduction to forensic science, 6th edn. Upper Saddle River, NJ: Prentice Hall, 1998.
24. Stoner D, Zeldes I. Speedometer examination—an aid in accident investigation. FBI L Enforcement Bull 1980;49:11–5.
25. Dalmotas DJ, German A, Consulting DJD. Crash pulse analysis using event data recorders. Proceedings of the 19th Canadian Multidisciplinary Road Safety Conference; 2009 June 8–10. Saskatoon, SK, Canada: The Canadian Association of Road Safety Professionals, 2009.
26. Liu S, Yin Z, Zhao H. Investigation of the cavitation and pressure change of brain tissue based on a transparent head model in its decelerating impact. J Mech Med Biol 2010;10:361–72.

Additional information and reprint requests:
Prof. Zhiyong Yin, Ph.D.
State Key Laboratory of Vehicle NVH and Safety
Research Institute for Traffic Medicine
Chongqing Key Laboratory of Vehicle/Biological Crash Security
Department 4, Institute of Surgery Research
Daping Hospital, Third Military Medical University
Chongqing 400042
China
E-mail: taodaiqin@hotmail.com